Supplement of Atmos. Chem. Phys., 20, 4889–4904, 2020
https://doi.org/10.5194/acp-20-4889-2020-supplement

Supplement of

Optical properties and molecular compositions of water-soluble and water-insoluble brown carbon (BrC) aerosols in northwest China

Jianjun Li et al.

Correspondence to: Qi Zhang (dkwzhang@ucdavis.edu) and Gehui Wang (ghwang@geo.ecnu.edu.cn)

Estimation of contribution of parent-PAHs and OPAHs to the light absorption of water-insoluble BrC

Average mass absorption coefficient of individual PAH (parent-PAH or OPAH) ($MAC_{PAH,AV}$) in the wavelength range of 300-700 nm in this study is cited from Samburova et al. (Samburova et al., 2016) and Huang et al. (Huang et al., 2018), who use authentic standard to measure the absorption of each individual PAH, and then calculated the $MAC_{PAH,AV}$ by multiplying MAC_{λ} of individual PAHs with the power distribution of the solar spectrum and spectrally integrated (eq S1).

$$MAC_{PAH,AV} = \frac{\int_{300}^{700} MAC_{\lambda} \times I_0(\lambda) d_{\lambda}}{\int_{300}^{700} I_0(\lambda) d_{\lambda}} \qquad (eq\ S1)$$

where $I_0(\lambda)$ is the clear sky Air Mass 1 Global Horizontal solar irradiance (Levinson et al., 2010). Then the $MAC_{PAH,AV}$ were used to calculated the contribution of individual PAH to solar-spectrum-weighed absorption coefficient of WI-BrC.

Estimation of light absorption of elemental carbon

The light absorption of elemental carbon (EC) were estimated by the output data of thermal/optical carbon analyzer, which is similar to the determination of black carbon (BC) light absorption by Aethalometer(Ram and Sarin, 2009). At first, the optical-attenuation (ATN) at wavelength of 632 nm (wavelength used in carbon analyzer) caused by EC is governed by the Beer-Lambert's law, according to the eq S2.

$$ATN_{632,EC} = -\ln\left(\frac{I}{I_0}\right) \qquad (eq\ S2)$$

where I_0 and I is the intensity of incident light and transmitted light through the filter substrate and aerosols.

Then $b_{ap,632,EC}$ can be obtained after correcting the multiple scattering and shadowing effects following by eq S4:

$$b_{ap,632,EC} = \frac{ATN_{632,EC}}{C \times R(ATN)} \times \frac{A}{V} \qquad \text{(eq S3)}$$

where A is the effective filter area (414 cm^2), *V* is the volume of air sampled (m3). *C* depends on absorbing material, mixing state of aerosols, and filter substrate, and a value of 2.14 was suggested for quartz filters (Weingartner et al., 2003;Bond and Bergstrom, 2006). *R*(ATN) is determined by eq S4:

$$\mathrm{R(ATN)} = \left(\frac{1}{f} - 1\right) \times \frac{lnATN_{632,EC} - ln10\%}{ln50\% - ln10\%} + 1 \qquad (eq\ S4)$$

where f is set as 1.103 for wintertime and 1.114 for summertime(Sandradewi et al., 2008).

At last, light absorption coefficient of EC at wavelength of λ ($b_{ap,\lambda,EC}$) can be calculated by eq S5:

$$b_{ap,\lambda,EC} = b_{ap,632,EC} \times \left(\frac{632}{\lambda}\right)^{AAE} \qquad \text{(eq S5)}$$

where AAE is the absorption Ångström exponent of EC. Previous study suggested that AAE of EC is in the range of 0.8 and 1.4(Lack et al., 2013), and a value of 1.0

were used in this study.

Then the contribution of BrC relative to EC ($f_{BrC/EC}$, %) can be calculated by eq S6:

$$f_{BrC/EC} = \frac{\int I_0(\lambda)(1-e^{-b_{ap,\lambda,BrC} \times h_{ABL}})d_\lambda}{\int I_0(\lambda)(1-e^{-b_{ap,\lambda,EC} \times h_{ABL}})d_\lambda} \times 100 \qquad \text{(eq S6)}$$

Table S1 Average (±1σ) values Abs and MAC of WS-BrC and WI-BrC at the wavelength of 340 nm, 350 nm, 360 nm, 370 nm, and 380 nm in the $PM_{2.5}$ aerosols from the rural site of Guanzhong Basin.

	340 nm		350 nm		360 nm		370 nm		380 nm	
	Summer	Winter	Summer	Winter	Summer	Winter	Summer	Winter	Summer	Winter
$Abs_{WS\text{-}BrC}$ (Mm^{-1})	6.55±1.91	27.5±12.4	5.55±1.61	23.36±10.6	5.27±1.36	20.7±9.02	4.34±1.17	17.8±7.59	3.55±0.99	15.07±6.41
$Abs_{WI\text{-}BrC}$ (Mm^{-1})	4.22±2.67	33.6±20.5	3.61±2.3	28.0±17.1	3.19±2.04	23.9±14.61	2.87±1.81	20.1±12.4	2.63±1.64	17.5±10.8
$MAC_{WS\text{-}BrC}$ ($m^2\ g^{-1}$)	1.29±0.22	1.29±0.34	1.10±0.19	1.09±0.29	1.05±0.18	0.97±0.26	0.87±0.15	0.85±0.23	0.71±0.13	0.71±0.2
$MAC_{WI\text{-}BrC}$ ($m^2\ g^{-1}$)	2.60±1.42	1.46±0.51	2.23±1.24	1.21±0.42	1.97±1.11	1.03±0.35	1.79±1.00	0.87±0.29	1.64±0.92	0.76±0.25

Table S2 Molecular concentrations of the measured parent-PAHs, OPAHs, nitrophenols, and isoprene and α-/*β*-pinene derived products in the $PM_{2.5}$ samples in the rural site of Northwest China during summer and winter.

	Summer			Winter		
	Average	Daytime	Nighttime	Average	Daytime	Nighttime
(a) parent-PAHs						
phenanthrene	0.68±0.33	0.64±0.39	0.73±0.26	6.67±3.78	5.64±2.02	7.7±4.73
anthracene	0.05±0.01	0.05±0.01	0.05±0.02	0.38±0.14	0.38±0.14	0.38±0.14
fluoranthene	0.36±0.13	0.36±0.12	0.37±0.14	5.92±3.29	5.68±2.78	6.15±3.71
pyrene	0.34±0.12	0.36±0.14	0.32±0.1	5.84±3.4	5.4±2.6	6.28±4
benz(a)anthracene	0.29±0.13	0.33±0.13	0.26±0.12	5.39±4.18	4.09±2.25	6.69±5.15
chrysene / triphenylene	0.61±0.23	0.63±0.23	0.58±0.22	9.55±6.35	8.32±4.5	10.78±7.57
benzo(b)fluoranthene	1.33±0.87	1.76±1.03	0.9±0.31	13.88±9.11	11.8±6.07	15.96±10.97
benzo(k)fluoranthene	0.38±0.24	0.51±0.28	0.26±0.09	3.51±2.24	3.03±1.52	3.98±2.69
benzo(e)pyrene	1.06±0.65	1.38±0.74	0.74±0.31	8.43±5.56	7.23±3.77	9.63±6.7
benzo(a)pyrene	0.66±0.45	0.94±0.47	0.39±0.17	5.21±3.7	4.23±2.28	6.19±4.5
perylene	0.13±0.09	0.19±0.09	0.07±0.03	1.12±0.85	0.84±0.45	1.39±1.04
indeno[123-cd]pyrene	1.41±1.23	2.24±1.27	0.58±0.2	7.72±5.55	6.65±3.55	8.79±6.83
dibenz(a,h)anthracene	0.25±0.17	0.34±0.18	0.16±0.09	1.77±1.38	1.49±0.84	2.05±1.71
benzo(ghi)perylene	1.25±0.98	1.91±1	0.58±0.23	6.95±4.87	6.06±3.24	7.85±5.95
(b) OPAHs						
anthraquinone	1.84±0.36	1.67±0.29	2.01±0.34	34.33±14.3	32.3±10.16	36.35±17.25
benzathrone	1.89±2.11	3.13±2.39	0.64±0.22	14.9±9.84	13.44±6.89	16.36±11.91
benzo(a)anthracene-7,12-dione	0.61±0.35	0.79±0.38	0.43±0.17	6.05±3.81	5.15±2.49	6.95±4.61
5,12-naphthacenequione	0.32±0.24	0.48±0.26	0.17±0.06	4.14±3.14	3.09±1.78	5.18±3.79
6H-benzo(cd)pyrene-6-one	9.33±11.44	16.95±12.05	1.72±0.67	38.84±29.42	35.42±19.46	42.26±36.45
(c) Nitrophenols						
4-nitrophenol	0.52±0.16	0.45±0.12	0.59±0.17	15.2±10.17	11.08±4.26	19.32±12.44
3-methyl-4-nitrophenol	BDL*	BDL	BDL	9.69±6.18	6.54±1.77	12.84±7.31
4-nitrocatechol	0.42±0.15	0.42±0.16	0.43±0.14	37.79±38.93	18.67±9.87	56.92±46.92
4-methyl-5-nitrocatechol	BDL	BDL	BDL	9.92±10.76	4.78±2.56	15.05±13.12
(d)Isoprene-derived products						
2-methylglyceric acid	4.15±1.35	3.58±1.04	4.73±1.38	BDL	BDL	BDL
2-methylthreitol	3.55±2.3	2.48±1.65	4.61±2.36	BDL	BDL	BDL
2-methylerythritol	10.84±6.31	8.9±5.65	12.79±6.33	BDL	BDL	BDL
(e) α-/β-Pinene derived products						
pinonic acid	3.92±0.97	3.35±0.68	4.5±0.88	BDL	BDL	BDL
pinic acid	3.85±0.96	3.8±0.54	3.9±1.24	BDL	BDL	BDL
3-methyl-1,2,3-butanetricarboxylic acid	14.27±6.38	18±6.16	10.53±3.94	BDL	BDL	BDL

*BDL: below detection limit.

Table S3 The solar-spectrum-weighed individual $MAC_{PAH,av}$, and the contributions of individual parent-PAH and OPAH to WI-BrC light absorption.

	$MAC_{PAH,av}$ (m^2 g^{-1})	Contribution to WI-BrC light absorption (%)			
		Summer		Winter	
		Daytime	Nighttime	Daytime	Nighttime
(a) parent-PAHs					
phenanthrene	0.0256 [a]	0.004±0.004	0.005±0.003	0.003±0.001	0.003±0.001
anthracene	0.2801 [a]	0.003±0.003	0.004±0.002	0.003±0.001	0.002±0.001
fluoranthene	0.2834 [a]	0.019±0.018	0.026±0.016	0.037±0.014	0.026±0.004
pyrene	0.353 [a]	0.021±0.018	0.028±0.016	0.044±0.016	0.032±0.006
benz(a)anthracene	0.2842 [a]	0.014±0.01	0.018±0.01	0.025±0.01	0.025±0.01
chrysene / triphenylene	0.0883 [a]	0.009±0.007	0.012±0.007	0.016±0.006	0.013±0.003
benzo(b)fluoranthene	0.3475 [a]	0.064±0.045	0.076±0.042	0.092±0.031	0.078±0.018
benzo(k)fluoranthene	0.3475 [b]	0.019±0.014	0.022±0.013	0.024±0.008	0.02±0.004
benzo(e)pyrene	0.7709 [c]	0.109±0.072	0.135±0.073	0.124±0.04	0.104±0.024
benzo(a)pyrene	0.7709 [a]	0.07±0.046	0.074±0.046	0.071±0.027	0.063±0.021
perylene	1.7942 [a]	0.032±0.02	0.032±0.02	0.033±0.014	0.032±0.012
indeno[123-cd]pyrene	1.0711 [d]	0.171±0.095	0.152±0.085	0.156±0.057	0.122±0.045
dibenz(a,h)anthracene	0.2842 [a]	0.027±0.014	0.025±0.013	0.024±0.009	0.019±0.006
benzo(ghi)perylene	0.1821 [a]	0.01±0.006	0.011±0.007	0.009±0.004	0.007±0.003
subtotal		0.57±0.35	0.62±0.34	0.66±0.23	0.55±0.15
(b) OPAHs					
anthraquinone	0.1032 [a]	0.037±0.03	0.051±0.025	0.083±0.023	0.064±0.017
benzathrone	0.4385 [a]	0.082±0.043	0.068±0.04	0.131±0.049	0.097±0.028
benzo(a)anthracene-7,12-dione	0.3069 [e]	0.028±0.02	0.032±0.019	0.036±0.014	0.032±0.006
5,12-naphthacenequione	0.3069 [a]	0.013±0.007	0.013±0.007	0.021±0.008	0.021±0.008
6H-benzo(cd)pyrene-6-one	0.4385 [f]	0.345±0.243	0.181±0.1	0.336±0.142	0.231±0.101
subtotal		0.51±0.28	0.34±0.19	0.61±0.21	0.44±0.13

[a] MAC_{PAH_av} values comes from Samburova et al. (2016) (Samburova et al., 2016); [b] use value from benzo(b)fluoranthene; [c] use value from benzo(a)pyrene; [d] use value from indeno[1,2,3-cd] fluoranthene; [e] use value from 5,12-naphthacenequione; [f] use value from benzathrone.

Table S3 The contribution (%) of detected individual nitrophenol to light absorption of water-soluble BrC at the wavelength of 365 nm.

	Summer			Winter		
	Average	Daytime	Nighttime	Average	Daytime	Nighttime
4-nitrophenol	0.06±0.02	0.04±0.01	0.07±0.02	0.41±0.16	0.32±0.13	0.49±0.14
3-methyl-4-nitrophenol	BDL[a]	BDL	BDL	0.28±0.13	0.20±0.06	0.36±0.13
4-nitrocatechol	0.06±0.02	0.05±0.01	0.07±0.02	1.30±1.16	0.66±0.25	1.93±1.35
4-methyl-5-nitrocatechol	BDL	BDL	BDL	0.46±0.43	0.23±0.10	0.68±0.50
Total nitrophenols	0.12±0.03	0.10±0.02	0.14±0.02	2.44±1.78	1.41±0.29	3.47±2.03

[a] BDL: below detection limit.

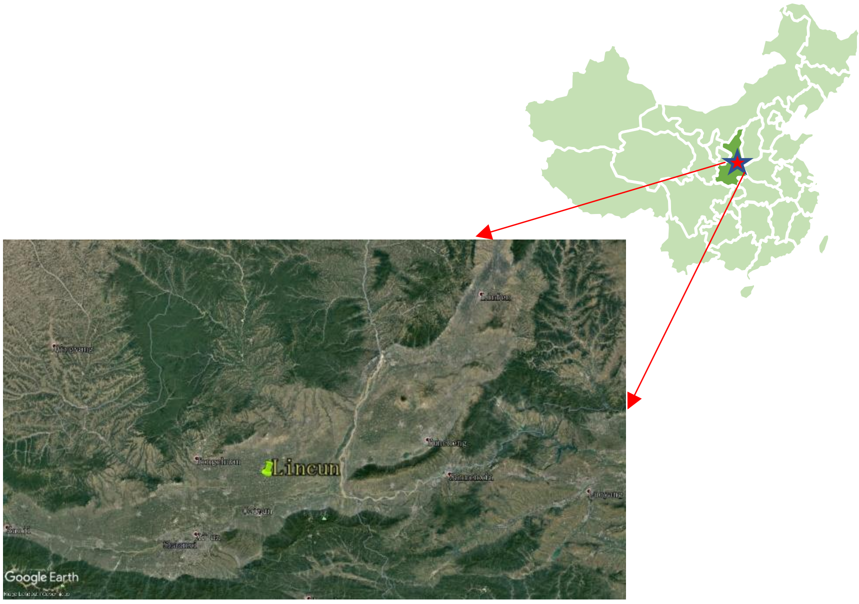

Figure S1 Location of the sampling site (Map data copyright @2019 Google).

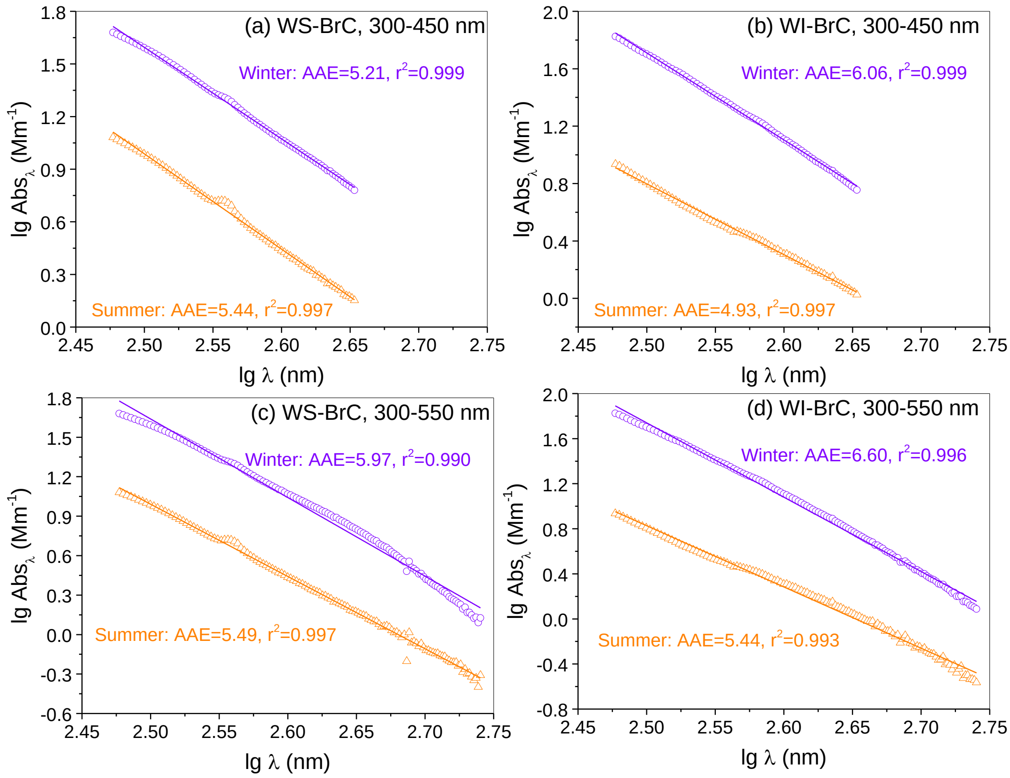

Figure S2 Comparison of Absorption Ångström exponent (AAE) calculation for average absorption spectrums in summer and winter in the wavelength of 300-450 nm (a and b) and 300-550 nm (c and d).

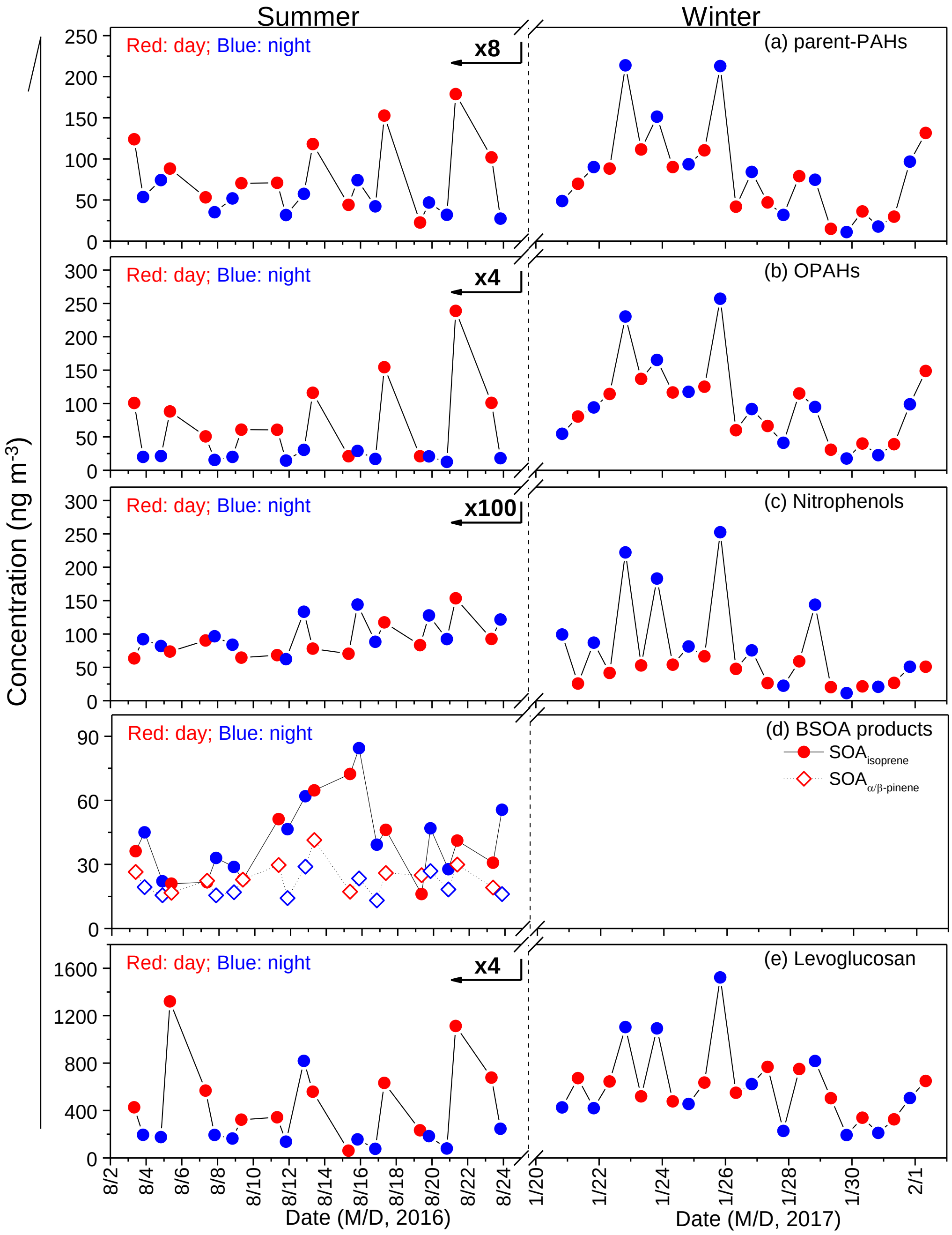

Figure S3 Temporal variation of subtotal concentrations of the measured parent-PAHs (a), OPAHs (b), nitrophenols (c), secondary products derived from isoprene ($SOA_{isoprene}$) and α-/β-pinene ($SOA_{\alpha\text{-}/\beta\text{-pinene}}$) (d), and levoglucosan (e) in $PM_{2.5}$.

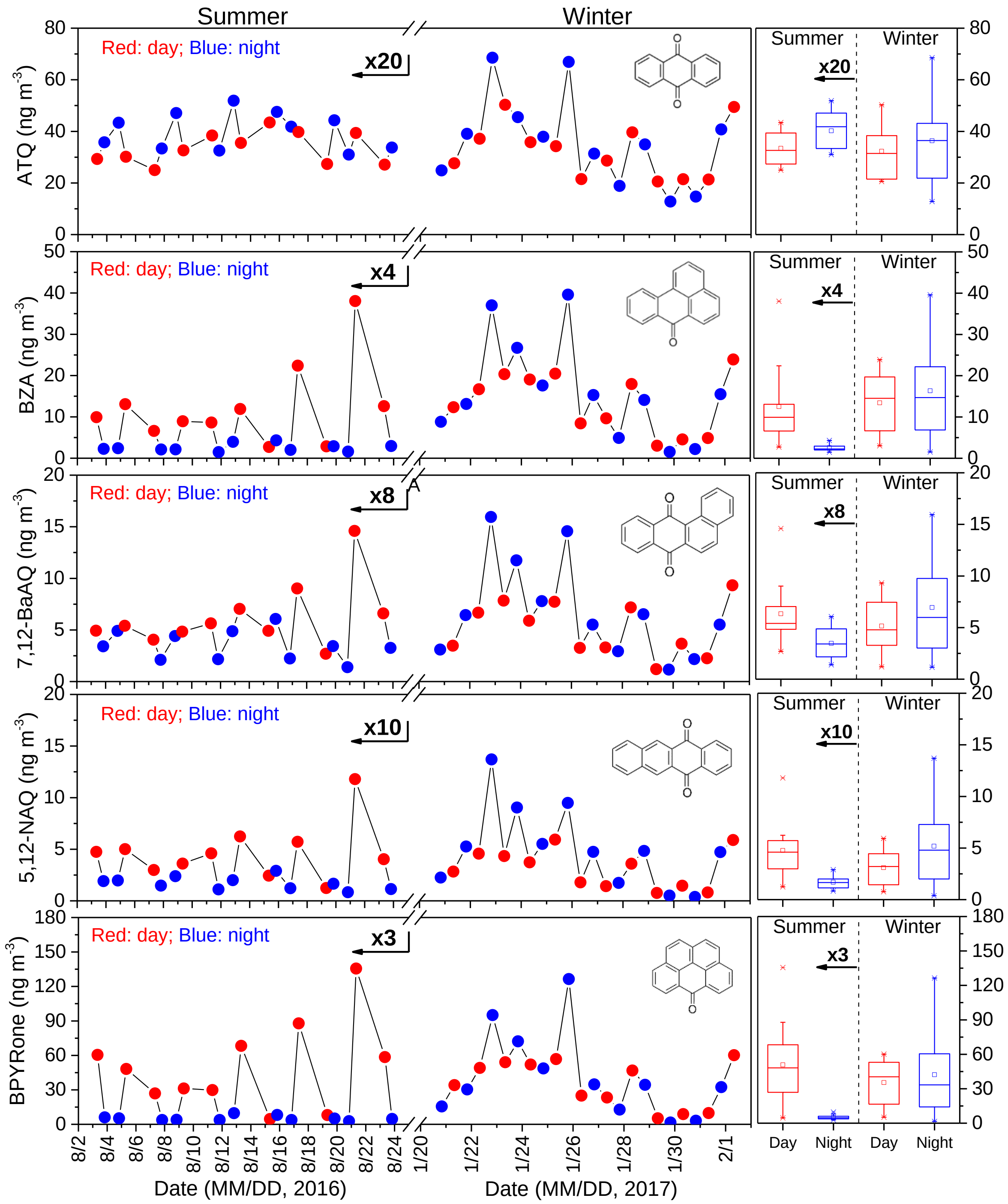

Figure S4 Time series and box charts of the five detected individual oxygenated-PAHs during the sampling period. The number of “×n” in the figures means summer concentrations were lower than winter data by a factor of n.

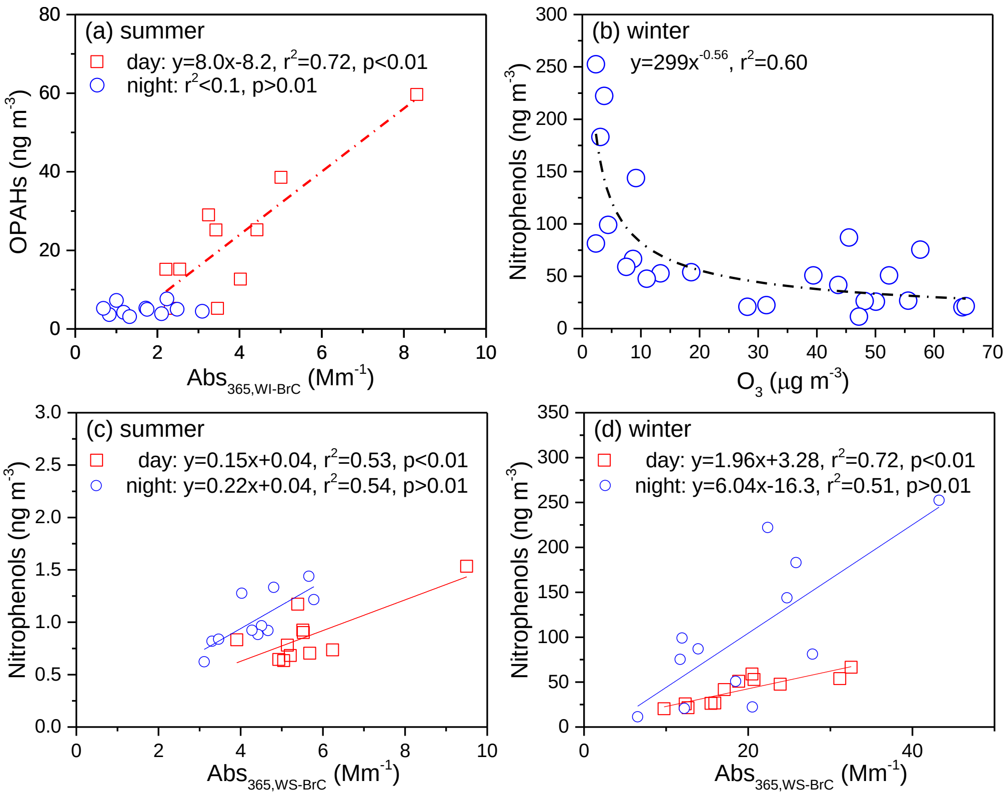

Figure S5 Relationships of OPAHs with $Abs_{365,WI-BrC}$ during daytime and nighttime in summer (a), nitrophenols with O_3 in winter (b), and nitrophenols with $Abs_{365,WS-BrC}$ during daytime and nighttime in summer (c) and winter (d).

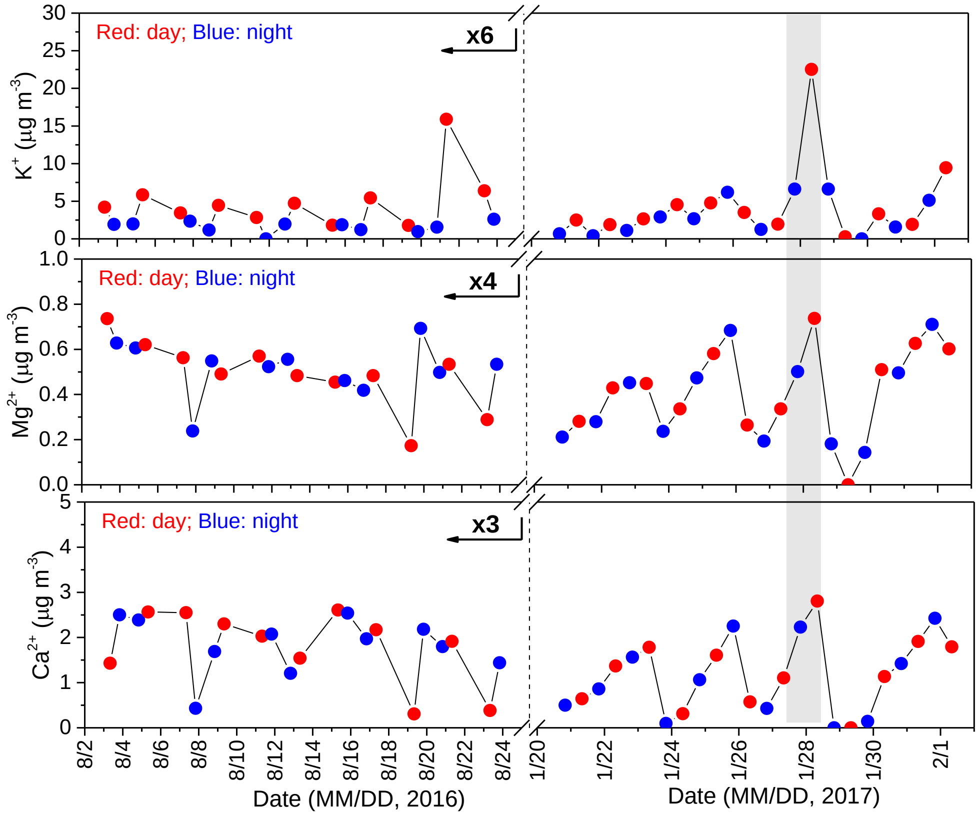

Figure S6 Temporal variation of water-soluble metal ions in $PM_{2.5}$ from the rural area of

Guanzhong Basin. Shadow denotes Chinese New Year eve and Spring festival, during which a large amount of fireworks were set off for celebration.

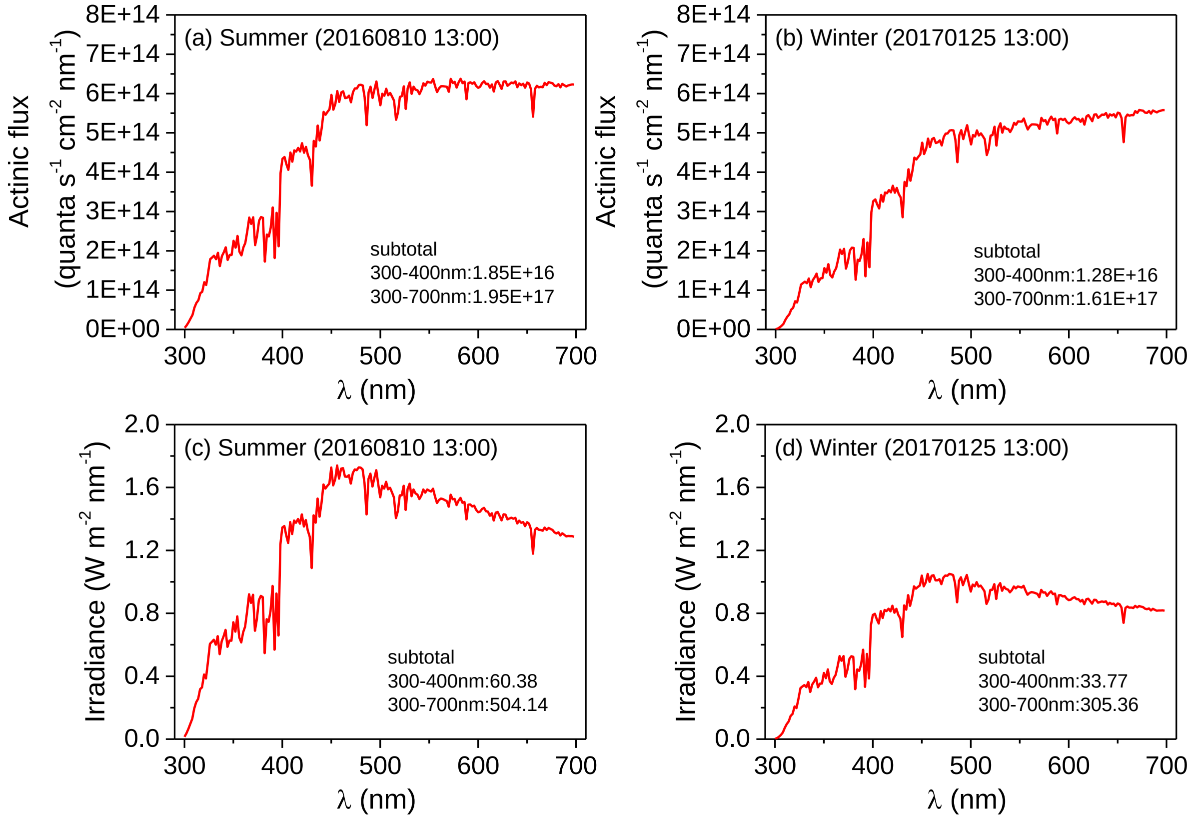

Figure S7 Total down-welling solar spectrum of actinic flux (a and b) and irradiance (c and d) at the sampling site at 20160810 13:00 and 20170125 13:00 (Beijing time) arrived. Data were provided by NCAR TUV Quick Calculator (http://cprm.acom.ucar.edu/Models/TUV/Interactive_TUV/), assuming no cloud effect. Ground elevation is 0.4 km a.s.l. (about 50 m above ground level).

Reference

Bond, T. C., and Bergstrom, R. W.: Light Absorption by Carbonaceous Particles: An Investigative Review, Aerosol Science and Technology, 40, 27-67, 10.1080/02786820500421521, 2006.

Huang, R.-J., Yang, L., Cao, J., Chen, Y., Chen, Q., Li, Y., Duan, J., Zhu, C., Dai, W., Wang, K., Lin, C., Ni, H., Corbin, J. C., Wu, Y., Zhang, R., Tie, X., Hoffmann, T., O'Dowd, C., and Dusek, U.: Brown Carbon Aerosol in Urban Xi'an, Northwest China: The Composition and Light Absorption Properties, Environ. Sci. Technol., 52, 6825-6833, 10.1021/acs.est.8b02386, 2018.

Lack, D. A., Bahreini, R., Langridge, J. M., Gilman, J. B., and Middlebrook, A. M.: Brown carbon absorption linked to organic mass tracers in biomass burning particles, Atmos. Chem. Phys., 13, 2415-2422, 10.5194/acp-13-2415-2013, 2013.

Levinson, R., Akbari, H., and Berdahl, P.: Measuring solar reflectance—Part I: Defining a metric that accurately predicts solar heat gain, Solar Energy, 84, 1717-1744, https://doi.org/10.1016/j.solener.2010.04.018, 2010.

Ram, K., and Sarin, M. M.: Absorption Coefficient and Site-Specific Mass Absorption Efficiency of Elemental Carbon in Aerosols over Urban, Rural, and High-Altitude Sites in India, Environ. Sci. Technol., 43, 8233-8239, 10.1021/es9011542, 2009.

Samburova, V., Connolly, J., Gyawali, M., Yatavelli, R. L. N., Watts, A. C., Chakrabarty, R. K., Zielinska, B., Moosmüller, H., and Khlystov, A.: Polycyclic aromatic hydrocarbons in biomass-burning emissions and their contribution to light absorption and aerosol toxicity, Science of The Total Environment, 568, 391-401, https://doi.org/10.1016/j.scitotenv.2016.06.026, 2016.

Sandradewi, J., Prévôt, A. S. H., Weingartner, E., Schmidhauser, R., Gysel, M., and Baltensperger, U.:

A study of wood burning and traffic aerosols in an Alpine valley using a multi-wavelength Aethalometer, Atmos. Environ., 42, 101-112, https://doi.org/10.1016/j.atmosenv.2007.09.034, 2008.

Weingartner, E., Saathoff, H., Schnaiter, M., Streit, N., Bitnar, B., and Baltensperger, U.: Absorption of light by soot particles: determination of the absorption coefficient by means of aethalometers, Journal of Aerosol Science, 34, 1445-1463, https://doi.org/10.1016/S0021-8502(03)00359-8, 2003.